Excitation Transfer in the Peridinin-Chlorophyll-Protein of *Amphidinium carterae*

Ana Damjanović, Thorsten Ritz, and Klaus Schulten
Department of Physics and Beckman Institute, University of Illinois at Urbana-Champaign, Urbana, Illinois 61801 USA

ABSTRACT Peridinin-chlorophyll-protein (PCP) is a unique light-harvesting protein that uses carotenoids as its primary light-absorbers. This paper theoretically investigates excitation transfer between carotenoids and chlorophylls in PCP of the dinoflagellate *Amphidinium carterae.* Calculations based on a description of the electronic states of the participating chromophores and on the atomic level structure of PCP seek to identify the mechanism and pathways of singlet excitation flow. After light absorption the optically allowed states of peridinins share their electronic excitation in excitonic fashion, but are not coupled strongly to chlorophyll residues in PCP. Instead, a gateway to chlorophyll Q_y excitations is furnished through a low-lying optically forbidden excited state, populated through internal conversion. Carbonyl group and non-hydrogen side groups of peridinin are instrumental in achieving the respective coupling to chlorophyll. Triplet excitation transfer to peridinins, mediated by electron exchange, is found to efficiently protect chlorophylls against photo-oxidation.

INTRODUCTION

About 40% of photosynthesis on earth occurs in aquatic environments. Aquatic photosynthetic systems exhibit a great genetic diversity comprising a dozen divisions, while all terrestrial plants are derived from a single class of a single division (Falkowski and Raven, 1997). This diversity is manifested in a large variety of photosynthetic apparatuses. Photosynthetic dinoflagellates, a class of phytoplankton that causes red tides and fish bite (Brown, 1997), possess a unique photosynthetic apparatus that extensively uses both carotenoids and chlorophylls (Chls) as the main light absorbers, as opposed to using mainly Chls. Most dinoflagellates use peridinin as their predominant carotenoid. Dinoflagellates contain a membrane-bound light-harvesting complex similar to that of higher plants (Kühlbrandt et al., 1994). In addition, they have developed a water-soluble antenna, peridinin-chlorophyll-protein (PCP), which has no sequence similarity with other known proteins (Norris and Miller, 1994). The structure of PCP of the species *Amphidinium carterae* (Hofmann et al., 1996), shown in Fig. 1, displays a carotenoid-to-chlorophyll ratio of 4:1, indicating the dominant role of carotenoids as light absorbers. Upon light absorption, peridinins in PCP convey their electronic excitation to Chl *a*. Estimates of the efficiency of this excitation transfer range from 88% (Bautista et al., 1999b) to more than 95% (Song et al., 1976; Krueger et al., submitted for publication). Chl *a* passes this excitation on to membrane-bound light-harvesting complexes and the photosystem II (PS-II).

Received for publication 27 December 1999 and in final form 20 June 2000.

Address reprint requests to Dr. Klaus Schulten, Dept. of Physics and Beckman Institute 3147, University of Illinois, 405 N. Mathews Ave., Urbana, IL 61801. Tel.: 217-244-1604; Fax: 217-244-6078; E-mail: kschulte@ks. uiuc.edu.

0006-3495/00/10/1695/11 $2.00

Besides the light-harvesting role, i.e., to provide the organism with energy necessary to drive its cellular reactions, carotenoids perform a secondary, but not less significant, role: they quench photo-oxidizing singlet oxygen and chlorophyll triplet excitations that arise as unwanted by-products of light-harvesting. The quenching reaction involves excitation transfer from chlorophyll to carotenoid triplet states.

Energy levels of peridinin and chlorophyll, the chromophores found in PCP, are depicted in Fig. 2. Two singlet excited states of carotenoids (S_1 and S_2) are energetically higher than and close to the Chl *a* Q_y and Q_x excitations, respectively. The excitation transfer might, thus, proceed through two pathways, i.e., $S_1 \rightarrow Q_y$ and $S_2 \rightarrow Q_x$. Due to significant resonance of the S_1 and Q_x states, excitation might also travel via an $S_1 \rightarrow Q_x$ pathway.

Light absorption by peridinin involves a strongly allowed transition from the ground state S_0 to the excited S_2 state with a 0-0 transition energy of 19,800 cm^{-1} (Akimoto et al., 1996), as measured in both methanol and in PCP. The S_2 states of peridinins are believed to couple excitonically, as suggested by circular dichroism (CD) spectra (Song et al., 1976). The interpretations of the CD spectra differ, however, favoring either a dimer (Song et al., 1976) or a tetramer (Pilch and Pawlikowski, 1998) exciton model. Excitonic states in other photosynthetic life forms, e.g., purple bacteria, are shown to play an important role in excitation transfer (Hu et al., 1997, 1998; Ritz et al., 1998; Damjanović et al., 2000).

The S_2 lifetime of peridinin in the organic solvents methanol or CCl_4 is equal to the time (τ_{AB}) for $S_2 \rightarrow S_1$ internal conversion. In PCP, however, there is an alternative route of relaxation from the S_2 state, namely $S_2 \rightarrow Q_x$ excitation transfer (transfer time τ_{AC}). The S_2 state lifetime in the solvent and in PCP was found to be ~190 fs (Akimoto et al., 1996), indicating absence or inefficiency of excitation transfer from this state. This follows from the well-known

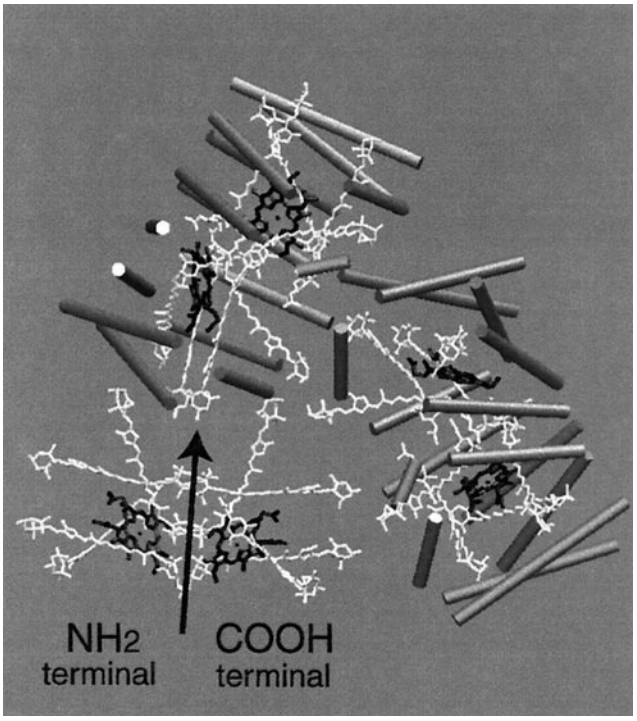

FIGURE 1 Structure of the PCP trimer of *A. carterae.* Chlorophylls (*black*) and peridinins (*white*) are in licorice representation, helices are represented as cylinders. The helices of one of the monomeric units are not shown in order to better display the arrangement of chromophores within a monomer; eight peridinins and two chlorophylls are organized into two almost identical domains, an NH_2-terminal domain and a COOH-terminal domain, related by a pseudo-symmetry axis (produced with the program VMD (Humphrey et al., 1996)).

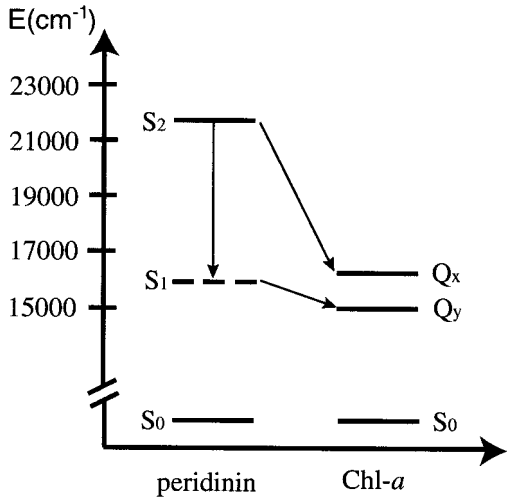

FIGURE 2 Excitation energies of peridinin and Chl states in PCP of *A. carterae.* The carotenoid states are labeled S_0 (ground state), S_1 (first excited state), and S_2 (second excited state). The respective chlorophyll states are labeled S_0, Q_y, and Q_x. Solid lines represent spectroscopically measured energy levels of peridinin and Chl; the dashed line indicates the estimated excitation energy of the S_1 state.

formula that describes the lifetime τ_A of a species A that can reach a state B ($A \rightarrow B$) or state C ($A \rightarrow C$) governed by reaction times τ_{AB} and τ_{AC}, respectively,

$$\tau_A = \tau_{AB}\tau_{AC}/(\tau_{AB} + \tau_{AC}). \quad (1)$$

In the case of $\tau_A = \tau_{AB}$ one can conclude $\tau_{AC} \gg \tau_{AB}$. Significant excitation transfer would have been marked by a shortening of the S_2 lifetime in the protein, compared to that in the solvent environment. One can state, therefore, that the S_2 state of peridinin relaxes into the lower-lying S_1 state, instead of passing its excitation to Chls.

The effectiveness of the $S_1 \rightarrow Q_y$ excitation transfer depends strongly on the electronic properties of the S_1 state. In general, the effectiveness increases with the strength of the $S_1 \rightarrow S_0$ transition dipole moment. The S_1 state in pure polyenes exhibits vanishing transition dipole moment due to two symmetries, a C_{2h} symmetry and an approximate alternancy symmetry (Pariser, 1956; Koutecky, 1966; Čižek et al., 1974). Obeying the C_{2h} point group, the polyene ground state S_0 and the first excited state S_1 transform according to A_g symmetry, while the S_2 state transforms according to B_u symmetry. This symmetry forbids the $S_0 \rightarrow S_1$ (i.e., $A_g \rightarrow A_g$) transition, while it allows the $S_0 \rightarrow S_2$ (i.e., $A_g \rightarrow B_u$) transition.

The alternancy symmetry arises from a topological feature of alternant hydrocarbons, according to which it is possible to divide unsaturated carbon atoms into two equivalent sets, "starred" (C*) and "unstarred" (C°) atoms, such that no two atoms of a set are joined by a chemical bond. The starred and unstarred atoms of $C_{20}H_{22}$ are displayed in Fig. 3 *a*. The presence of heteroatoms will break the alternancy symmetry. The alternancy symmetry is responsible for one-electron pairing properties of alternant hydrocarbons, i.e., molecular orbitals occur in pairs with energies ϵ_n and $-\epsilon_n + \epsilon$, where ϵ is the same constant for all orbitals. The one-electron pairing properties arise also for many-electron states: the many-electron wavefunctions of polyenes, according to the alternancy symmetry, are labeled "+" and "−", e.g., $1^1 A_g^-$ (S_0), $2^1 A_g^-$ (S_1), and $1^1 B_u^+$ (S_2), etc. The alternancy symmetry forbids optical transitions between states of same symmetry, i.e., transitions "+" → "+" and "−" → "−" (Damjanović et al., 1999). Consequently for polyenes, the $1^1 A_g^-$ (S_0) → $1^1 B_u^+$ (S_2) transition is allowed according to both C_{2h} and alternancy symmetry, while the $1^1 A_g^-$ (S_0) → $2^1 A_g^-$ (S_1) transition is forbidden according to both symmetries.

Carotenoids, however, do not exhibit the perfect symmetry of polyenes. In Fig. 3, *a* and *b* the chemical structure of peridinin is compared with that of the polyene $C_{20}H_{22}$; the methyl groups and other functional groups attached to the carbons of the conjugated π-electron system distinguish such carbons as heteroatoms, and effectively break the alternancy symmetry. The C_{2h} symmetry, in protein environments, is broken due to distortions, but is retained ap-

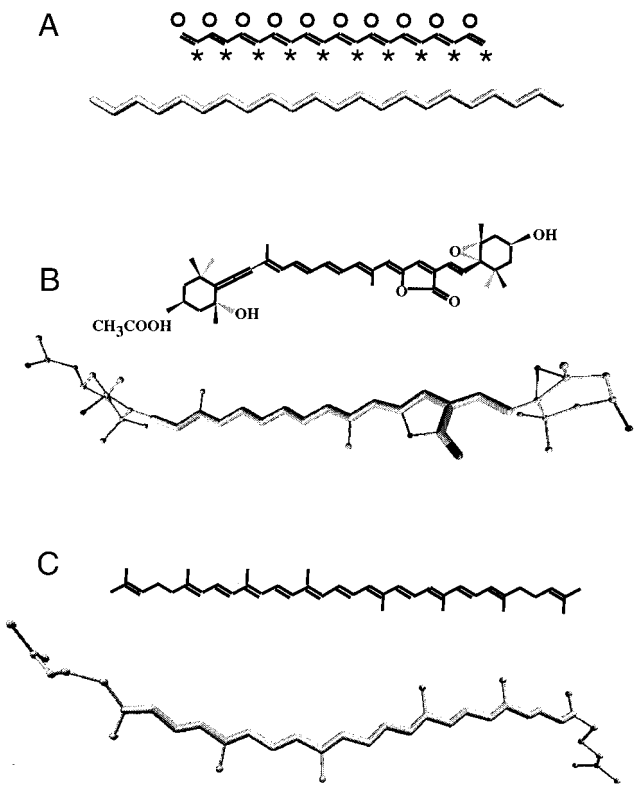

FIGURE 3 Comparison of polyene and carotenoid structures. (*a*) Chemical structure (*top*) and rendered representation (*bottom*) of the polyene $C_{20}H_{22}$ (hydrogen atoms not shown), chemical structure, and rendered representation not drawn to the same scale. The structure displays the C_{2h} rotational symmetry; alternately, symmetry is shown in labeling of conjugated carbon atoms as "starred" and "unstarred." (*b*) Chemical structure of peridinin and rendered representation of per611 in PCP (conjugated system is shown in licorice representation). The oxygen atoms are shown in black, methyl groups are shown as spheres. (*c*) Chemical structure of lycopene and rendered representation of the geometry of lycopene in LH2 of *Rhodospirillum molischianum.* The conjugated system is shown in licorice representation, methyl groups are shown as spheres. Rendered representations were produced with the program VMD (Humphrey et al., 1996).

proximately in the solution environment for some symmetric carotenoids, e.g., lycopene displayed in Fig. 3 *c*. For very asymmetric carotenoids, e.g., peridinin shown in Fig. 3 *b*, which possesses a carbonyl group in the conjugated π-electron system, both C_{2h} and alternancy symmetries are strongly broken, even in the solution environment.

Symmetry-breaking renders allowed electronic transitions that are forbidden in the perfectly symmetric case. The S_1 state requires breaking of both the alternancy symmetry and the geometrical C_{2h} symmetry to gain absorption strength. Both symmetries are broken in peridinin; however, despite the symmetry-breaking, the transition dipole moment of the peridinin S_1 state is believed to be small, as indicated by a lack of experimental evidence of S_1 state absorption in solution.

The emission of the peridinin S_1 state in solution was measured to lie between 12,804 cm^{-1} and 13,889 cm^{-1}, depending on the solvent (Mimuro et al., 1992; Bautista et al., 1999a). The S_1 lifetime of peridinin in solution depends strongly on the polarity of the solvent, ranging from 7 ps in strongly polar solvents to 172 ps in non-polar solvents (Bautista et al., 1999a). In PCP, the S_1 state lifetime could not be resolved by the time-correlated single-photon counting method and, thus, has been estimated to be shorter than the instrument response time of 3 ps (Akimoto et al., 1996). The authors in Bautista et al. (1999b) estimate the lifetime of the S_1 state in PCP to be 3.1 ps. These measurements suggest, according to Eq. 1, that the S_1 state provides a gateway for excitation transfer. Based on the rise time of Chl *a* bleaching, the peridinin $\rightarrow$ Chl *a* transfer time was estimated to be 3.2 ps (Bautista et al., 1999b). Recent measurements reported in Krueger et al. (submitted for publication) estimate the energy transfer time to be $\sim$2.4 ps.

The atomic level structure of PCP from *Amphidinium (A.) carterae* has recently become available through x-ray crystallography (Hofmann et al., 1996), thus opening the door to an explanation of the function of this protein through structure-based calculations. Due to the proximity of carotenoids and chlorophylls in light-harvesting complexes, their electronic couplings need to be described through the full Coulomb interaction (Coulomb mechanism) (Nagae et al., 1993; Krueger et al., 1998a; Damjanović et al., 1999), as opposed to the customary dipole-dipole term (Förster, 1948) only. Moreover, the proximity suggests that one considers also the electron exchange coupling (Dexter, 1953) for excitation transfer; the couplings decay exponentially with donor-acceptor distance, and may become significant at short distances. Triplet excitation transfer requires a change of spin in excitation-deexcitation processes, and can therefore proceed only through the exchange mechanism. Accordingly, proximity of donor and acceptor molecules is required for efficient triplet excitation transfer.

In the following we briefly describe the structure of PCP (Hofmann et al., 1996) and summarize the theoretical formalism used in calculations of electronic excitations of carotenoids and Chls, as well as couplings and transfer rates between them (Damjanović et al., 1999). We then present the pathways and mechanisms of excitation transfer in PCP suggested by the calculations.

STRUCTURE

Peridinin-chlorophyll *a*-protein forms a trimer of 48 helices that provide a scaffold for 24 peridinins and six chlorophylls. The trimeric structure is depicted in Fig. 1. In each monomer, eight peridinins and two chlorophylls are organized into two almost identical domains, an NH_2-terminal domain, and a COOH-terminal domain, related by a pseudo-symmetry axis. Fig. 4 shows the arrangement of four peridinins surrounding a chlorophyll in the NH_2-terminal domain.

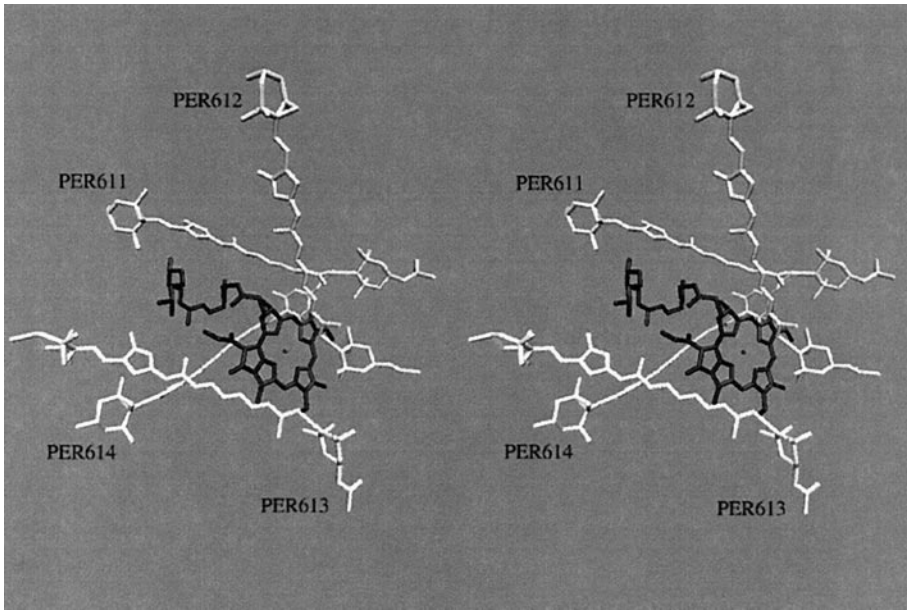

FIGURE 4 Stereo view of the four peridinins and a chlorophyll belonging to the NH_2-terminal domain (see Fig. 1). The representation of Chl includes its phytol tail; the tail is omitted in Fig. 1 (produced with the program VMD (Humphrey et al., 1996)).

THEORY

The rate of excitation transfer between donor *D* and acceptor *A*, according to Fermi's golden rule (Förster, 1948; Dexter, 1953) is,

$$k_{DA} = \frac{2\pi}{\hbar}|U_{DA}|^2 \int S_D(E) S_A(E) dE. \quad (2)$$

Here, U_{DA} is the electronic coupling between donor and acceptor, and $S_D(E)$ and $S_A(E)$ are defined (Davidovich and Knox, 1979; Agranovich and Galanin, 1982; Hu et al., manuscript in preparation) as

$$S_D(E) = \frac{f_D(E)}{E^3}\left(\int_{E=0}^{\infty} dE \frac{f_D(E)}{E^3}\right)^{-1}$$

$$S_A(E) = \frac{\varepsilon_A(E)}{E}\left(\int_{E=0}^{\infty} dE \frac{\varepsilon_A(E)}{E}\right)^{-1}. \quad (3)$$

Here $f_D(E)$ and $\varepsilon_A(E)$ are the normalized emission spectrum of the donor and the absorption molar extinction coefficient of the acceptor, respectively. In the following, $f_D(E)$ and $\varepsilon_A(E)$ are approximated by Gaussians $G(E_{D(A)}, \Gamma_{D(A)})$ with $E_{D(A)}$ the energy of the emission or absorption maximum, and $\Gamma_{D(A)}$ the full width at half-maximum, two parameters being estimated from spectroscopic data. Fluorescence from the S_1 state of peridinin in CS_2 has been measured (Mimuro et al., 1992) and yields E_D = 13,333 cm^{-1}, Γ_D = 3,200 cm^{-1}. Because the influence of the protein surrounding of peridinin in PCP is expected to be similar to that of polar solvents (Bautista et al., 1999a), we will use the E_D value measured in methanol, i.e., E_D = 13,870 cm^{-1}. Unfortunately, fluorescence from the S_2 state of peridinin has not been observed; based solely on the similarity between peridinin and β-carotene absorption spectra, we use values corresponding to the fluorescence spectrum of β-carotene in ethanol (Shreve et al., 1991), namely, E_D = 19,170 cm^{-1}, Γ_D = 3,500 cm^{-1}. For the S_1 state absorption we use E_A = 16,000 cm^{-1}, as suggested in Akimoto et al. (1996), and we assume Γ_A = 3,200 cm^{-1} (the same as for the S_1 state emission). The S_2 state absorption spectrum in PCP we approximate, rather crudely, as a Gaussian with E_A = 21,739 cm^{-1} and Γ_A = 4,315 cm^{-1}. The Gaussian parameters to describe the Chl *a* absorption were determined from measurements of the PCP absorption spectrum in Akimoto et al. (1996) as E_D = 14,992 cm^{-1}, Γ_D = 291 cm^{-1} for the Q_y state, and E_D = 16,129 cm^{-1}, Γ_D = 1,041 cm^{-1} for the Q_x state. The spectral overlap integrals $\int S_D(E)\, S_A(E)\, dE$ are then evaluated as 0.45 eV^{-1} ($S_2 \rightarrow Q_x$), 0.08 eV^{-1} ($S_2 \rightarrow Q_y$), 1.31 eV^{-1} ($S_1 \rightarrow Q_y$), 0.42 ($S_1 \rightarrow Q_x$), 0.79 eV^{-1} ($S_1 \rightarrow S_1$), 0.69 eV^{-1} ($S_2 \rightarrow S_2$). A value of 1 eV^{-1} is assumed for the spectral overlap integral between triplet excited states, as suggested in Nagae et al. (1993).

The electronic coupling U_{DA} between chromophores, cf. Eq. 2, can be split into two additive contributions

$$U_{DA} = U^{c}_{DA} + U^{ex}_{DA}, \quad (4)$$

corresponding to a direct Coulomb and an electron exchange term (Förster, 1948; Dexter, 1953). Following Damjanović et al. (1999) these terms can be expanded

$$U^{c(ex)}_{DA} = \sum_{\substack{i,j \\ \in I_D}} \sum_{\substack{R,S \\ \in I_A}} C^{c(ex)}_{ij,RS} \times \langle \Psi^*_D | {}^{sm}O^{i}_{j} | \Psi_D \rangle \times \langle \Psi_A | {}^{s-m}O^{R}_{S} | \Psi^*_A \rangle, \quad (5)$$

where I_D and I_A denote the set of atomic orbital indices of the donor and acceptor molecules, and $C^{c(ex)}_{ij,RS}$ describes the Coulomb or exchange integrals involving atomic orbitals labeled by *i*, *j*, *R*, and *S*. The spin tensor operators ${}^{sm}\hat{O}^{i}_{j}$, ${}^{s-m}\hat{O}^{R}_{S}$ prompt the intramolecular transitions $|\Psi_D\rangle \rightarrow |\Psi^*_D\rangle$, $|\Psi_A\rangle \rightarrow |\Psi^*_A\rangle$ between the ground and singlet excited states of donor and acceptor. Coulomb interaction does not involve spin change (s = 0), while electron exchange can proceed between singlet and triplet states, and is described by the spin tensor operators ${}^{sm}\hat{O}^{i}_{j}$ and ${}^{s-m}\hat{O}^{i}_{j}$ of singlet (rank s = 0) and triplet type (rank s = 1), respectively.

The Coulomb integral $C^{c}_{ij,RS}$ can be approximated (Nagae et al., 1993) as $S_{ij}(e^2/R_{ij,RS})\, S_{RS}$, where S_{ij} and S_{RS} denote atomic-orbital overlap integrals, and $R_{ij,RS}$ is the distance between the midpoint of atoms *i* and *j* and the midpoint of atoms *R* and *S*. The transition densities are placed at atomic centers and at midpoints between atomic centers; unfortunately, this procedure neglects the spatial distribution of the π orbitals, and a simple $1/r$ dependence to model the Coulomb interaction might be an oversimplification.

The exchange integrals $C^{ex}_{ij,RS}$ have been calculated as described in Damjanović et al. (1999) by accounting for the contribution of the bridge atoms (hydrogen and carbon atoms bonded to the conjugated system) to the

exchange interaction. Hydrogen atoms of peridinin and chlorophyll, not resolved in the crystal structure of PCP (Hofmann et al., 1996), were added using the program QUANTA (MSI, 1997). Fig. 5 depicts peridinin and chlorophyll atoms belonging to the conjugated π-system as well as the bridge atoms.

We used the value $n = 1$ for the refractive index in our calculations. It is not clear which value of n would be the most appropriate for the particular protein surrounding peridinin and Chl in PCP. The influence of protein on pigment charge distributions could, in principle, be studied by quantum chemistry calculations. In case of a dipole-dipole interaction, the Förster rate of energy transfer scales with n as $(1/n^2)[(n^2 + 2)/3]^4$ (Agranovich and Galanin, 1982). For $n = 1.6$ (the value estimated for PCP (Kleima et al., 2000a)) the latter scaling factor is 0.81; for $n = 1$ the scaling factor is 1.0. We therefore believe that a choice of $n = 1$ does not result in a significant error.

The transition density matrix elements $\langle \Psi_D^* | {}^{sm}\hat{O}_j^i | \Psi_D \rangle$ and $\langle \Psi_A | {}^{sm}\hat{O}_S^R | \Psi_A^* \rangle$ in (Eq. 5) (Nagae et al., 1993; Damjanović et al., 1999) and the wavefunctions of carotenoid and Chl excited electronic states were described through a semi-empirical Pariser-Parr-Pople, self-consistent field, configuration interaction (PPP-SCF-CI) method. The Pariser-Parr-Pople (PPP) Hamiltonian (Pariser and Parr, 1953; Pople, 1953)

$$H = \sum_{i<j} Z_i Z_j R_{ij} + \sum_{i,\sigma} \left(-I_i - \sum_{j \neq i} Z_j R_{ij} \right) n_{i\sigma} + \sum_{i \neq j,\sigma} t_{ij} c_{i\sigma}^{+} c_{j\sigma} + \frac{1}{2} \sum_{i,j,\sigma,\tilde{\sigma}} R_{ij} n_{i\sigma} n_{i\tilde{\sigma}} \quad (6)$$

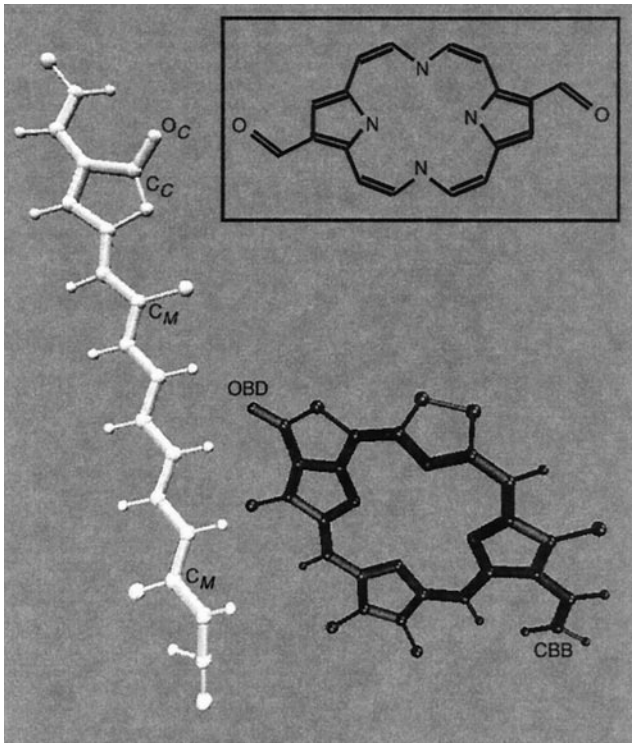

FIGURE 5 Peridinin and chlorophyll models used in our calculations: the conjugated systems of per613 (*white*) and chl601 (*black*) are shown in licorice representation. Carbon and hydrogen atoms bonded to the conjugated systems are shown as spheres (produced with the program VMD (Humphrey et al., 1996)). The *inset* shows the conjugated system of the symmetric chlorophyll analog used to calculate transition density matrix elements.

involves orbitals of π-type only. $c_{i\sigma}^{+}$ and $c_{j\sigma}$ are creation and annihilation operators acting on the mutually orthogonal atomic π-orbitals; the operator $n_{i\sigma} = c_{i\sigma}^{+} c_{i\sigma}$ is the corresponding number operator; R_{ij} is the effective electron-electron repulsion integral between an electron in atomic orbital at site i and one in orbital at site j; t_{ij} is the resonance integral between atoms i and j; I_i is the effective ionization potential of an orbital at site i; Z_i is the net charge of the core at atom i which was chosen as $Z_i = 1$.

The empirical expression for t_{ij} and the Ohno formula for R_{ij} in (Eq. 6) are provided in Table 1. The semi-empirical parameters for the PPP Hamiltonian are also listed in Table 1. The parameters for carbon, oxygen, and nitrogen have been taken from Dewar and Morita (1969). The carbons with methyl groups attached to them have been denoted as C_M. To determine parameters for heteroatom C_M, we exploit the relationship between the valence state ionization potentials of a heteroatom X (I_X), and of a trigonal $2p\pi$ carbon orbital (taken as $I_C(p) = 11.16$ eV in our calculations), with the so-called Coulomb parameter for this heteroatom, h_X (Leach, 1967), defined as

$$h_X = [(I_X - I_C(p))/I_C(p)](\alpha/\beta). \quad (7)$$

Here parameters α and β are -7.2 eV and -3.0 eV, respectively (Leach, 1967). The Coulomb parameter for C_M ranges from $h_M = -0.3$ to $h_M = -0.5$ (Leach, 1967); for our calculations we choose the value $h_M = -0.3$. This yields a value for I_M of 9.76 eV. Exploiting an approximate proportionality between $I_k^{1/2}$ and R_{kk} (Dewar and Morita, 1969) we estimate for the latter a value of 10.41 eV (see Table 1).

A (PPP-SCF-CI) calculation, including single and double (S + D) excited π-electron configurations, was performed for singlet states of peridinins and Chl. The (S + D) basis is necessary for a description of the carotenoid S_1 state, since this state is dominated by doubly excited configurations (Schulten and Karplus, 1972; Tavan and Schulten, 1986). To describe chromophore triplet states we used singly (S) excited π-electron configurations only.

Electronic structure calculations were performed for crystal structure geometries (Hofmann et al., 1996) of the four peridinins shown in Fig. 4, i.e., per611, per612, per613, and per614. Chlorophyll electronic structure calculations are based on geometries of a symmetric chlorophyll analog, the structure of which is displayed in Fig. 5, *inset.* The analog is symmetric about the magnesium atom; it does not possess the double bond of ring II which is present in Chls, and the CBB atom of Chl (which is indicated in Fig. 5) is treated as an oxygen atom. For the PPP-SCF-CI calculations performed on the analog structure, the Q_x and the Q_y states are easily identified. For the calculations performed instead on the real Chl structure, the electronic states mix, and it is impossible to identify them. We believe that the error arising from modeling of chlorophylls with a symmetric analog is insignificant compared to systematic errors that are reflected in transition dipole moments (see below).

RESULTS AND DISCUSSION

We present here only results for calculations on chromophores belonging to the NH_2-terminal cluster, expecting that, due to a pseudo-symmetry of the COOH and the NH_2 terminal cluster (see Fig. 1), the qualitative conclusions drawn from our calculations will also hold for the COOH-terminal cluster.

Peridinin symmetry and peridinin models

The effect of symmetry breaking on the S_1 state transition dipole moment and excitation transfer from this state is investigated through three parametrizations of the PPP Hamiltonian. The first set of parameters treats all the atoms

TABLE 1 Expressions for t_{ij} and R_{ij} featured in Eq. 6

$$t_{ij} = -2.43 \text{ eV} + 3.21 \text{ eV } (r_{ij} - 1.397\text{Å})$$
$$R_{ij} = 14.397 \text{ eV} \times [(2 \times 14.397 \text{ eV}/(R_{ii} + R_{jj}))^2 + r_{ij}^2/\text{Å}^2]^{-1/2}$$

Carbon (C)	Carbonyl Carbon (C_C)	Methyl Carbon (C_M)	Carbonyl Oxygen (O_C)	Nitrogen (N)
$I_k = 11.16$	$I_k = 12.29$	$I_k = 9.76$	$I_k = 16.02$	$I_k = 14.12$
$R_{kk} = 11.13$	$R_{kk} = 11.68$	$R_{kk} = 10.41$	$R_{kk} = 14.49$	$R_{kk} = 12.34$

Here r_{ij} is the distance between the nuclear sites i and j. Also presented are parameters of the PPP Hamiltonian, as defined in Eq. 6, expressed in eV.

belonging to the conjugated system of peridinin as carbon atoms (e.g., the oxygen atom is treated as a carbon). Since there are no heteroatoms, alternancy symmetry applies to this idealized model. The second parametrization distinguishes heteroatoms O_C and C_C. These atoms are indicated in the peridinin structure shown in Fig. 5. The third parametrization treats O_C and C_C, as well as C_M, as heteroatoms, and is therefore, in principle, the most realistic. Even more realistic calculations of peridinin electronic states would also account for the allene group and the lactone ring. However, we are not aware of available parametrizations of these chemical groups, and at the moment we neglect them in our description.

The first, second, and third parametrization will be referred to as "symmetric," "no methyl," and "methyl" parametrizations, respectively. The increased symmetry breaking in going from "symmetric" to the "methyl" parametrization is expected to result in an increase of the S_1 state transition dipole moment and its coupling to the chlorophyll excitations. By comparing the transfer times calculated with the three parametrizations, we seek to demonstrate the role of symmetry breaking in achieving fast, i.e., efficient, energy transfer.

Transition dipole moments of peridinin states

Table 2 displays transition dipole moments of per611, per612, per613, and per614 S_1 and S_2 states, calculated with the three parameter sets. As expected, the transition dipole moment of the S_1 state for the "symmetric" parameter set vanishes, to the level of accuracy of our calculations. The "no methyl" and "methyl" parametrizations result in non-vanishing transition dipole moments of the S_1 state, due to intensity borrowing from the allowed S_2 state through symmetry breaking. Because the symmetry is broken more strongly in the "methyl" parameter set than in the "no-methyl" parametrization, the calculated S_1 transition dipole moments are largest for the "methyl" parametrization. In parallel, the S_2 transition dipole moments decrease in going from the "symmetric" to the "no-methyl" to the "methyl" parametrization.

TABLE 2 Transition dipole moments (in Debye) of peridinins, calculated with three parameter sets, "symmetric," "no methyl," and "methyl" (see text)

Carotenoid (State)	Symmetric	No Methyl	Methyl
per611 S_1	1.47×10^{-3}	0.17	4.70
per612 S_1	1.55×10^{-3}	0.18	4.70
per613 S_1	1.65×10^{-3}	0.36	5.08
per614 S_1	1.74×10^{-3}	0.08	4.56
per611 S_2	15.45	15.08	14.00
per612 S_2	15.43	14.84	13.84
per613 S_2	15.37	15.11	13.50
per614 S_2	15.62	15.00	13.50

The quality of the "methyl" parametrization has been tested for lycopene. Lycopene has methyl sidegroups, but no other sidegroups that break the polyene symmetry, and its geometry in LH2 from *Rhodospirillum molischianum* is known. The transition dipole moments of the S_1 and S_2 transitions have been estimated from the emission spectra of these states (Zhang et al., 2000). Our calculations with the "methyl" parametrization reproduce the experimentally measured transition dipoles within 20%, suggesting that the methyl parametrization approximates the excited state wavefunctions well.

The values of transition dipole moments of S_2 peridinin states in PCP were estimated in the range 10.6–12.4 Debye (D) (Carbonera et al., 1999), suggesting that our calculated S_2 state transition dipole moments that lie between 13.5 and 14.0 D are slightly too large. The S_1 emission of peridinin has been observed (Mimuro et al., 1992); however, its S_1 absorption in solution has not been observed. An estimate of the order of magnitude of the upper bound of the transition dipole moment for a transition that is not detectable in absorption spectroscopy can be obtained from measurements on neurosporene in LH2 from *Rhodobacter sphaeroides*. Neurosporene S_1 absorption cannot be detected, but the S_1 transition dipole moment has been estimated from comparison between S_1 and S_2 fluorescence spectra to be 0.86 D (Zhang et al., 2000). This measurement shows that transitions with transition dipole moments of around 1 D can still be undetectable in absorption spectroscopy. One expects that the S_1 transition of peridinin is allowed more than the neurosporene S_1 transition, because peridinin is more asymmetric than neurosporene. The "no-methyl" parametrization for peridinin yields S_1 transition dipole moment values between 0.08 D and 0.36 D (cf. Table 2), i.e., values that are smaller than the estimated value for the transition dipole moment of neurosporene. A more accurate description of symmetry breaking, through the "methyl"

parametrization, yields a rather large value of the S_1 state transition dipole moments for peridinin, namely between 4.56 D and 5.08 D (cf. Table 2). Interestingly, a large value of the S_1 state transition dipole moment in PCP, of about 3 D, was also suggested from a recent polarized transient absorption measurement (Krueger et al., submitted for publication).

Transition dipole moments of chlorophyll states

The magnitude of the Chl Q_y state transition dipole moment is calculated to be 10.5 D. This value, obtained with the (S + D)-CI method, is closer to the experimentally estimated value of 5.2 D in vacuum (Kleima et al., 2000b) than our previously reported value of 14.3 D (Damjanović et al., 1999), obtained with the S-CI method.

The magnitude of the Chl Q_x state transition dipole moment calculated with the (S + D)-CI method is 2.3 D. The Chl*a* Q_x transition dipole moment in PCP of *A. carterae* has not been measured directly; however, the ratio between Q_x and Q_y transition dipole moments in PCP of *Symbiodinium kawagutii* has been estimated from the absorption spectrum (Iglesias-Prieto et al., 1991). Assuming that the same ratio applies to PCP of *A. carterae,* we estimate the Q_x dipole moment to be 3.5 D.

For both Q_y and Q_x states the calculated transition dipole moments differ significantly from the experimentally measured values, indicating that the excited state wavefunctions have not been approximated well, although we now use a more extensive basis set than in our earlier calculations (Damjanović et al., 1999). This implies that the absolute carotenoid-Chl transfer times evaluated in the present study bear a significant error.

Mechanism of excitation transfer

Tables 3 and 5 provide couplings and transfer times for excitation transfer through the Coulomb and exchange mechanisms, respectively. As in the case of carotenoid-bacteriochlorophyll interactions in LH2 of the purple bacteria (Scholes et al., 1997; Damjanović et al., 1999), all exchange couplings are weaker than the respective Coulomb couplings. The strongest exchange coupling arising between per613 and chl601 is of the order of 10^{-4} eV, which is one order of magnitude smaller than the corresponding Coulomb coupling. As analyzed in Damjanović et al. (1999), the method used to evaluate the exchange coupling rather overestimates than underestimates the couplings, due to use of Gaussian-type orbitals. Because even the strongest (per613-chl601) exchange coupling results in a transfer time that is two orders of magnitude longer than the corresponding Coulomb transfer time, we can safely conclude that the Coulomb mechanism dominates the peridinin $\rightarrow$ chlorophyll excitation transfer.

S_2 excitons

Our calculations suggest very strong couplings between the S_2 states of peridinins within the NH_2-terminal cluster. The respective couplings, presented in Table 4 ("methyl" parametrization), lie between 0.0165 eV (133 cm^{-1}) and 0.0648 eV (523 cm^{-1}). Our findings confirm the experimental suggestion in Song et al. (1976) of the existence of S_2 excitons. Couplings between S_1 states of peridinins are weaker, being only of the order of 10^{-3} eV, thus making excitonic interactions insignificant.

Spreading of the S_2 excitation among the four peridinins is followed by a rapid relaxation to the S_1 state. The probability of excitation of the S_1 state of a particular peridinin is determined by the density of the S_2 exciton on that peridinin. The latter density depends on the interplay between coupling strengths, site energies, and structural and thermal disorder. To estimate the exciton density, we construct an effective Hamiltonian describing the S_2 excitons (couplings are given in units of cm^{-1})

$$\hat{H} = \begin{pmatrix} \epsilon_1 & 523 & 204 & 236 \\ 523 & \epsilon_2 & 248 & 133 \\ 204 & 248 & \epsilon_3 & 303 \\ 236 & 133 & 303 & \epsilon_4 \end{pmatrix}. \quad (8)$$

The basis vectors are $|1\rangle = |$per611* per612 per613 per614$\rangle$, $|2\rangle = |$per611 per612* per613 per614$\rangle$, etc (per611* indi-

TABLE 3 Coulomb couplings (in eV) and transfer times between peridinin and chlorophyll singlet states, evaluated for three parameter sets "symmetric," "no methyl," and "methyl," as defined in the text

	Symmetric		No Methyl		Methyl	
Carotenoid (State)-Chl (state)	U_{DA}	t_{DA}	U_{DA}	t_{DA}	U_{DA}	t_{DA}
per611 S_1-chl601 Q_y	2.34×10^{-6}	14.4 μs	1.17×10^{-3}	58.0 ps	-1.91×10^{-2}	218 fs
per612 S_1-chl601 Q_y	2.64×10^{-4}	1.14 ns	-7.86×10^{-4}	128 ps	8.79×10^{-3}	1.02 ps
per613 S_1-chl601 Q_y	1.16×10^{-3}	58.5 ps	3.58×10^{-3}	6.19 ps	1.64×10^{-2}	196 fs
per614 S_1-chl601 Q_y	-1.44×10^{-3}	38.1 ps	1.12×10^{-3}	63.1 ps	2.30×10^{-2}	150 fs
per611 S_2-chl601 Q_x	5.47×10^{-3}	7.73 ps	5.19×10^{-3}	8.64 ps	4.75×10^{-3}	10.3 ps
per612 S_2-chl601 Q_x	3.45×10^{-3}	19.5 ps	-3.07×10^{-3}	24.7 ps	-2.90×10^{-3}	27.8 ps
per613 S_2-chl601 Q_x	3.11×10^{-3}	24.1 ps	-2.58×10^{-3}	34.9 ps	-1.61×10^{-3}	88.9 ps
per614 S_2-chl601 Q_x	8.06×10^{-3}	3.59 ps	-7.02×10^{-3}	4.72 ps	-6.70×10^{-3}	5.20 ps

TABLE 4 Coulomb couplings (in eV) and transfer times between different peridinin singlet states, evaluated for three parameter sets "symmetric," "no methyl," and "methyl," as defined in the text

Carotenoid (state)-Chl (state)	Symmetric		No Methyl		Methyl	
	U_{DA}	t_{DA}	U_{DA}	t_{DA}	U_{DA}	t_{DA}
per611 S_1-per612 S_1	-1.11×10^{-5}	1.08 μs	-3.45×10^{-5}	111 ns	-8.43×10^{-3}	1.87 ps
per611 S_1-per613 S_1	1.84×10^{-6}	39.0 μs	1.01×10^{-6}	129 μs	-3.44×10^{-3}	11.2 ps
per611 S_1-per614 S_1	4.94×10^{-7}	544 μs	4.62×10^{-6}	6.22 μs	-3.49×10^{-3}	10.9 ps
per612 S_1-per613 S_1	-1.25×10^{-6}	84.7 μs	2.47×10^{-5}	218 ns	4.02×10^{-3}	8.21 ps
per612 S_1-per614 S_1	-3.36×10^{-6}	11.7 μs	-1.38×10^{-5}	680 ns	2.04×10^{-3}	32.0 ps
per613 S_1-per614 S_1	3.30×10^{-6}	12.2 μs	-3.57×10^{-3}	10.4 ps	4.93×10^{-3}	5.45 ps
per611 S_2-per612 S_2	7.76×10^{-2}	25.2 fs	-7.29×10^{-2}	28.6 fs	-6.48×10^{-2}	36.1 fs
per611 S_2-per613 S_2	3.16×10^{-2}	152 fs	-3.03×10^{-2}	165 fs	-2.53×10^{-2}	238 fs
per611 S_2-per614 S_2	3.68×10^{-2}	112 fs	-3.45×10^{-2}	128 fs	-2.93×10^{-2}	177 fs
per612 S_2-per613 S_2	3.98×10^{-2}	95.8 fs	3.72×10^{-2}	110 fs	3.07×10^{-2}	161 fs
per612 S_2-per614 S_2	2.10×10^{-2}	339 fs	1.96×10^{-2}	396 fs	1.65×10^{-2}	551 fs
per613 S_2-per614 S_2	4.84×10^{-2}	65.0 fs	4.65×10^{-2}	70.5 fs	3.76×10^{-2}	108 fs

cates that per611 is in the excited S_2 state). The couplings between S_2 states of peridinins are those presented in Table 4, converted into units of cm^{-1}. The S_2 exciton density ρ_i on peridinin i is calculated using Meier et al. (1997)

$$\rho_i = Z^{-1} \sum_n c_{i,n}^2 \exp(-E_n/kT),$$
$$Z = \sum_n \exp(-E_n/kT). \quad (9)$$

Here E_n are excitonic energies and $c_{i,n}$ are coefficients arising in the expansion of excitonic states, as obtained from diagonalization of the Hamiltonian (Eq. 8). The excitonic states are assumed to be populated according to the Boltzmann distribution at the temperature of 300 K.

The S_2 exciton densities ρ_i depend sensitively on the site energies ϵ_i. We assume four models for the site energies ϵ_i. In the first model (model A), all site energies are set to 19,800 cm^{-1} (Akimoto et al., 1996). In the second model (model B) we use different site energies for different peridinins; this difference arises in natural systems due to different protein environments of the four peridinins. Carbonera et al. (1999) have assigned the excitation energies 18,400 cm^{-1}, 20,600 cm^{-1}, 19,300 cm^{-1}, and 18,700, to per611, per612, per613, and per614, respectively, based on the fit of the PCP absorption spectrum; we therefore use ϵ_1 = 18,400 cm^{-1}, ϵ_2 = 20,600 cm^{-1}, ϵ_3 = 19,300 cm^{-1}, and ϵ_4 = 18,700. In the third and fourth models, we take disorder into account by varying the site energies according to a Gaussian distribution, with maxima assigned as in the second model, and widths of 200 cm^{-1} (model C, case of a weak disorder) and 1,000 cm^{-1} (model D, case of a strong disorder).

The calculated exciton densities for the four models of ϵ_i are shown in Table 6. The exciton densities presented for models C and D are averages over samples including 1000 random selections. Evidently, the site energies ϵ_i strongly influence the exciton density ρ_i. Per611 has the lowest site energy and therefore the highest exciton density, while per612 has the highest site energy and the lowest exciton density. The effect of static and dynamic disorder is to reduce the asymmetry among the four peridinins and distribute the excitation more equally among them. However, even for a relatively strong disorder of 1000 cm^{-1}, the exciton density on per612 remains low.

TABLE 5 Exchange couplings (in eV) and transfer times between peridinin and Chl singlet and triplet states. The couplings were calculated with the "methyl" parametrization (see text)

Carotenoid-Chl (State)	Coupling	Transfer Time
per611 S_1-chl601 Q_y	-4.62×10^{-6}	3.72 μs
per612 S_1-chl601 Q_y	4.68×10^{-6}	3.63 μs
per613 S_1-chl601 Q_y	-1.68×10^{-4}	2.82 ns
per614 S_1-chl601 Q_y	1.00×10^{-5}	794 ns
per611 S_2-chl601 Q_x	-1.13×10^{-6}	182 μs
per612 S_2-chl601 Q_x	1.01×10^{-6}	228 μs
per613 S_2-chl601 Q_x	-1.51×10^{-4}	10.2 ns
per614 S_2-chl601 Q_x	6.24×10^{-6}	6.09 μs
per611 T-chl601 T	1.11×10^{-5}	851 ns
per612 T-chl601 T	-1.12×10^{-5}	836 ns
per613 T-chl601 T	5.93×10^{-4}	298 ps
per614 T-chl601 T	3.70×10^{-5}	76.6 ns

TABLE 6 Excitation densities ρ_i, as calculated from Eq. 9, for the four models (see text) of excitation energies ϵ_i. The electron densities presented for models C and D are averages over samples including 1000 random selections

Peridinin	Model A	Model B	Model C	Model D
per611	0.37	0.86	0.71	0.47
per612	0.36	0.03	0.03	0.04
per613	0.14	0.02	0.03	0.18
per614	0.13	0.19	0.23	0.30

$S_2 \rightarrow Q_x$ transfer

The calculated coupling energies between the S_2 states of peridinins and the chlorophyll Q_x state, presented in Table 3, lie between 1.6 meV and 6.7 meV for the "methyl" parameter set. The respective times for the $S_2 \rightarrow Q_x$ excitation transfer, determined from Eqs. 2 and 5, range from 5.2 ps (per614) to 88.9 ps (per613), and are also given in Table 3. The calculated transition dipole moment of the Q_x state is a factor of 1.5 smaller than the measured value, suggesting that our calculated transfer times are too long. An additional uncertainty arises through the choice of the S_2 emission spectrum of β-carotene with an emission maximum at 19,170 cm^{-1}. This assumption results in a spectral overlap of 0.45 eV^{-1}. A rather dramatic shift of the emission maximum to 17,170 cm^{-1} would result in a spectral overlap of $\sim$1.89 eV^{-1}, and a reduction of transfer times by about a factor of four. However, even this dramatic shift in the spectral overlap would not change the conclusions of our calculations, i.e., that there is no or very little excitation transfer via the $S_2 \rightarrow Q_x$ route. The internal conversion between S_2 and S_1 states occurs within 190 fs, which is nearly two orders of magnitude shorter than the shortest calculated transfer time.

$S_1 \rightarrow Q_y$ transfer

The $S_1 \rightarrow Q_y$ transfer times, calculated with the "methyl" parameter set and presented in Table 3, range from 150 fs (per614) to 1.0 ps (per612). These transfer times are all shorter than the experimentally estimated transfer times of 3.2 ps (Bautista et al., 1999b) and 2.4 ps (Krueger et al., submitted for publication). This discrepancy stems from errors in the calculated U_{DA} value, and from uncertainties in the spectral overlap integral (e.g., from the Gaussian approximation for the absorption and emission spectra). The error in the U_{DA} values might arise from the overestimate of the Q_y transition dipole moment by a factor of two, and limited accuracy of parameters used to describe carbons with methyl groups (as discussed above).

Interestingly, the "symmetric" parameter set for per613 and per614 yields transfer times of the order of tens of picoseconds, as indicated in Table 3. The dipole-dipole term does not contribute to the transfer due to the forbidden character of the S_1 state in this case. The results reveal that the higher-order multipole (quadrupole, etc.) interactions contribute to an energy transfer as fast as 38 ps and 58 ps.

As expected, Table 3 confirms that the $S_1 \rightarrow Q_y$ transfer times calculated with the "no methyl" parameter set are shorter than those calculated with the "symmetric" parameter set, but longer than those calculated with the "methyl" parametrization. The "no methyl" transfer times, ranging from 6.2 ps (per613) to 128 ps (per612) are competing with the S_1 state lifetime, which is probably of the order of tens of picoseconds in the polar environment of PCP (Bautista et al., 1999a). We can, thus, conclude that the symmetry breaking through the carbonyl group only is not strong enough to achieve the nearly unit efficiency of energy transfer observed in PCP; such high efficiency is achieved through a combination of symmetry breaking through the carbonyl and through the methyl groups.

Photoprotection by carotenoids

Triplet excitations of chlorophyll *a* in PCP are efficiently quenched by the four closest peridinins. Table 5 presents couplings and times for chlorophyll $\rightarrow$ peridinin triplet excitation transfer. Compared to the lifetime of chlorophyll triplet states of $\sim$10 μs, transfer times ranging from $\sim$300 ps to 850 ns secure an efficient excitation transfer and, hence, indicate excellent photoprotection.

CONCLUSIONS

The presented results give a comprehensive description of the pathways of excitation transfer processes in PCP following initial absorption of a photon. These pathways are depicted schematically in Fig. 6. Due to excitonic interactions between the S_2 states, light absorption results in an excitation of all four peridinins within one cluster of a subunit (e.g., per611, per612, per613, per614). This S_2 excitation is not shared equally by all four peridinins, but resides mostly on per611, per613, and per614, and not much on per612. The reason for the low S_2 exciton density on per612 is the comparatively high site energy of per612.

Direct $S_2 \rightarrow Q_x$ excitation transfer is inefficient compared to internal conversion of the S_2 state into the optically forbidden S_1 state. The calculated electronic couplings and spectral overlaps suggest transfer rates that are slow compared to internal conversion and, thus, confirm earlier experimental observations. Because of the low S_2 exciton density on per612, internal conversion occurs only to the S_1 states of per611, per613, and per614, as indicated in Fig. 6. The S_1 states of the different peridinins are only weakly coupled among each other and do not form an exciton state. After internal conversion, excitation is therefore localized in the S_1 states of per611, per613, or per614. As pointed out in Desamero et al. (1998) the S_1 state has a high spectral overlap with both Q_x and Q_y states of Chl *a*, proposing that both $S_1 \rightarrow Q_x$ and $S_1 \rightarrow Q_y$ transfer pathways can be utilized. The calculated couplings for $S_1 \rightarrow Q_x$ transfer range from 5.0×10^{-4} eV to 2.6×10^{-3} eV ("methyl" parametrization) and are, thus, small compared to the couplings for $S_1 \rightarrow Q_y$ transfer (cf. Table 3). We therefore conclude that $S_1 \rightarrow Q_y$ transfer is the major pathway of excitation transfer from the S_1 state. Inspecting the couplings from all four peridinins reveals that the S_1-Q_y coupling between per612 and Chl is considerably weaker than the S_1-Q_y coupling among the other three peridinins and

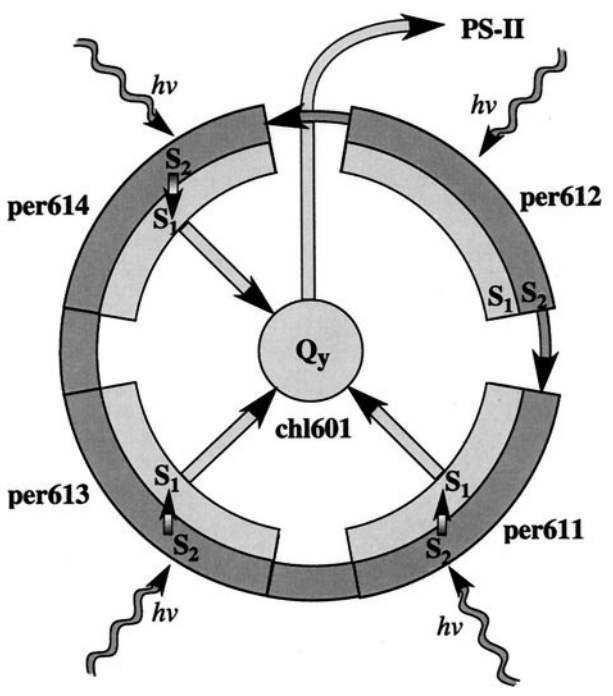

FIGURE 6 Scheme of singlet excitation transfer and energy funneling in PCP. Shown are the representative chromophores belonging to the NH_2 terminus of a PCP monomeric unit (see Figs. 1 and 4, and text): four peridinins (per611, per612, per613, per614) and a chlorophyll (chl601). Through light-absorption peridinins are excited into their S_2 states, which are excitonically coupled among all four peridinins. Per611, per613, and per614 retain the energy and convert it to their respective S_1 excitations. Excitation of the S_1 state of per612 is prevented, since the occupancy of its S_2 state is low. The S_1 states are not excitonically coupled, but transfer individually to the Q_y state of chl601. The latter state transfers its energy from PCP to photosystem II (PS-II).

Chl. Interestingly, because of the low participation of per612 in the S_2 exciton state as discussed above, transfer through the per612 S_1 state is avoided, thus enhancing the overall Car → Chl transfer efficiency. We are not aware of any other light-harvesting system in which a similarly intricate interplay between S_2 excitation energies and S_1-Q_y coupling strengths has been demonstrated.

Comparison of light-harvesting strategies in PCP and LH2

It is instructive to compare the strategies for excitation transfer between carotenoids and Chls in PCP of the dinoflagellate *A. carterae* with that in LH2 of purple bacteria (Krueger et al., 1998b; Damjanović et al., 1999). In both proteins, Coulomb couplings rather than exchange couplings dominate the carotenoid → Chl singlet excitation transfer, but exchange couplings efficiently quench chlorophyll triplet excitations. The efficiencies and pathways of singlet excitation transfer, however, differ between the two proteins.

In LH2 of the purple bacterium *Rhodopseudomonas acidophila,* the overall transfer efficiency was measured to be only 38% (Angerhofer et al., 1995). Rhodopin glucoside, found in LH2 of *Rps. acidophila,* has the same number of double bonds as lycopene found in LH2 of the purple bacterium *Rs. molischianum,* and one can speculate that both bacteria exhibit similar, i.e., low, efficiency of carotenoid → BChl excitation transfer. However, carotenoid → Chl excitation transfer in PCP is highly efficient, with an overall efficiency of 88% (Bautista et al., 1999b) to 100% (Song et al., 1976).

The carotenoids found in LH2 of *Rs. molischianum* and *Rps. acidophila,* lycopene and rhodopin, glucoside mainly use the S_2 state to transfer excitation to BChls (Krueger et al., 1998b; Damjanović et al., 1999). This route is inherently inefficient because excitation transfer competes with extremely fast internal conversion. Due to the high symmetry of the chromophores, which results in weak couplings between S_1 and Q_y states (Ritz et al., accepted for publication), efficiency of $S_1 \rightarrow Q_y$ transfer is also low.

Peridinin in PCP of *A. carterae* overcomes this problem by not relying on $S_2 \rightarrow Q_x$ transfer. It opts instead on using the S_1 state, which lives longer than the S_2 state and furnishes, thus, a more likely pathway for efficient excitation transfer, provided that the couplings between the S_1 and Q_y states are strong. The strong couplings between S_1 and Q_y states in peridinin are achieved through symmetry breaking by carbonyl and methyl groups of peridinin. To achieve the high efficiency of energy transfer and light-harvesting, nature has chosen a highly asymmetric carotenoid to be the main light-absorber in PCP.

Evolution of photosynthetic life forms has resulted in rather divergent strategies for light harvesting, as reviewed, for example, in Hu et al. (1998), even though carotenoids and chlorophylls are mainly used as chromophores. This divergence provides ample opportunities to learn from nature through comparison of physical principles it exploits in the first step of photosynthesis, light-harvesting. As more light-harvesting proteins become structurally resolved, a prerequisite for any physical analysis, we will gain an improved understanding of one of the most critical aspects of life on earth: harnessing the energy of the sun.

The authors thank Stefania Lampoura, Brent Krueger, and Rienk van Grondelle for communication of data and useful discussions.

This work was supported by National Science Foundation Grants NSF BIR 94-23827 EQ and NSF BIR-9318159, National Institutes of Health Grant NIH PHS 5 P41 RR05969-04, and the Roy J. Carver Charitable Trust.

REFERENCES

Agranovich, V. M., and M. D. Galanin. 1982. Electronic Excitation Energy Transfer in Condensed Matter. North-Holland Publishing Company, Amsterdam.

Akimoto, S., S. Takaichi, T. Ogata, Y. Nishimura, I. Yamazaki, and M. Mimuro. 1996. Excitation energy transfer in carotenoid-chlorophyll pro-

tein complexes probed by femtosecond fluorescence decays. *Chem. Phys. Lett.* 260:147–152.

Angerhofer, A., F. Bornhäuser, A. Gall, and R. Cogdell. 1995. Optical and optically detected magnetic resonance investigation on purple bacterial antenna complexes. *Chem. Phys.* 194:259–274.

Bautista, J. A., R. E. Connors, B. B. Raju, R. G. Hiller, F. P. Sharples, D. Gosztola, M. Wasielewski, and H. A. Frank. 1999a. Exited state properties of peridinin: observation of solvent dependence of the lowest excited singlet state lifetime and spectral behavior unique among carotenoids. *J. Phys. Chem. B.* 103:8751–8758.

Bautista, J., R. Hiller, F. Sharples, D. Gosztola, M. Wasielewski, and H. Frank. 1999b. Singlet and triplet transfer in the peridinin-chlorophyll *a*-protein from *Amphidinium carterae. J. Phys. Chem. A.* 103: 2267–2273.

Brown, K. 1997. *Pfiesteria:* on the molecular biology of a sea monster. *J. NIH Res.* 9:26–27.

Carbonera, D., G. Giacometti, U. Segre, E. Hofmann, and R. G. Hiller. 1999. Structure-based calculations of the optical spectra of the light-harvesting peridinin-chlorophyll-protein complexes from *Amphidinium carterae* and *Heterocapsa pygmaea. J. Phys. Chem. B.* 103:6349–6356.

Čižek, J., J. Paldus, and I. Hubač. 1974. Correlation effects in the low-lying excited states of PPP models of alternant hydrocarbons. I. Qualitative rules for the effect of limited configuration interaction. *Int. J. Quantum Chem.* 8:951–970.

Damjanović, A., T. Ritz, and K. Schulten. 1999. Energy transfer between carotenoids and bacteriochlorophylls in a light harvesting protein. *Phys. Rev. E.* 59:3293–3311.

Damjanović, A., T. Ritz, and K. Schulten. 2000. Excitation energy trapping by the reaction center of *Rhodobacter sphaeroides. Int. J. Quantum Chem.* 77:139–151.

Davidovich, M. A., and R. S. Knox. 1979. On the rate of triplet excitation transfer in the diffusive limit. *Chem. Phys. Lett.* 68:391–394.

Desamero, R., V. Chynwat, I. van der Hoef, F. Jansen, J. Lugtenburg, D. Gosztola, M. Wasielewski, A. Cua, D. Bocian, and H. Frank. 1998. Mechanism of energy transfer from carotenoids to bacteriochlorophyll: light-harvesting by carotenoids having different extents of π-electron conjugation incorporated in the B850 antenna complex from the carotenoidless bacterium *Rhodobacter sphaeroides* R-26.1. *J. Phys. Chem. B.* 102:8151–8162.

Dewar, M. J. S., and T. Morita. 1969. Ground states of conjugated molecules. XII. Improved calculations for compounds containing nitrogen and oxygen. *J. Am. Chem. Soc.* 91:796–801.

Dexter, D. 1953. A theory of sensitized luminescence in solids. *J. Chem. Phys.* 21:836–850.

Falkowski, P., and J. Raven. 1997. Aquatic photosynthesis. Blackwell, Malden, MA.

Förster, T. 1948. Zwischenmolekulare Energiewanderung und Fluoreszenz. *Ann. Phys. (Leipzig).* 2:55–75.

Hofmann, E., P. Wrench, F. Sharples, R. Hiller, W. Welte, and K. Diederichs. 1996. Structural basis of light harvesting by carotenoids: peridinin-chlorophyll-protein from *Amphidinium carterae. Science.* 272:1788–1791.

Hu, X., A. Damjanović, T. Ritz, and K. Schulten. 1998. Architecture and function of the light harvesting apparatus of purple bacteria. *Proc. Natl. Acad. Sci. USA.* 95:5935–5941.

Hu, X., T. Ritz, A. Damjanović, and K. Schulten. 1997. Pigment organization and transfer of electronic excitation in the purple bacteria. *J. Phys. Chem. B.* 101:3854–3871.

Humphrey, W. F., A. Dalke, and K. Schulten. 1996. VMD—visual molecular dynamics. *J. Mol. Graphics.* 14:33–38.

Iglesias-Prieto, R., N. Govind, and R. Trench. 1991. Apoprotein composition and spectroscopic characterization of the water-soluble peridinin-chlorophyll *a*-proteins from three symbiotic dinoflagellates. *Proc. R. Soc. Lond. B. (Bio. Sci.).* 246:275–283.

Kleima, F. J., E. Hofmann, B. Gobets, I. H. M. van Stokkum, R. van Grondelle, K. Diederichs, and H. van Amerongen. 2000a. Förster excitation energy transfer in peridinin-chlorophyll-*a*-protein. *Biophys. J.* 78:344–353.

Kleima, F. J., M. Wendling, E. Hofmann, E. J. G. Peterman, R. van Grondelle, and H. van Amerongen. 2000b. Peridinin chlorophyll *a* protein: relating structure and steady-state spectroscopy. *Biochemistry.* 39:5184–5195.

Koutecky, J. 1966. Contribution to the theory of alternant systems. *J. Chem. Phys.* 44:3702–3706.

Krueger, B. P., G. D. Scholes, and G. R. Fleming. 1998a. Calculation of couplings and energy-transfer pathways between the pigments of LH2 by the ab initio transition density cube method. *J. Phys. Chem. B.* 102:5378–5386.

Krueger, B., G. Scholes, R. Jimenez, and G. Fleming. 1998b. Electronic excitation transfer from carotenoid to bacteriochlorophyll in the purple bacterium *Rhodopseudomonas acidophila. J. Phys. Chem. B.* 102: 2284–2292.

Kühlbrandt, W., D. Wang, and Y. Fujiyoshi. 1994. Atomic model of plant light-harvesting complex by electron crystallography. *Nature.* 367: 614–621.

Leach, H. 1967. Electronic Absorption Spectra and Geometry of Organic Molecules. Academic Press, New York.

Meier, T., Y. Zhao, V. Chernyak, and S. Mukamel. 1997. Polarons, localization, and excitonic coherence in superradiance of biological antenna complexes. *J. Chem. Phys.* 107:3876–3893.

Mimuro, M., U. Nagashima, S. Takaichi, Y. Nishimura, I. Yamazaki, and T. Katoh. 1992. Molecular structure and optical properties of carotenoids for the in vivo energy transfer function in the algal photosynthetic pigment system. *Biochim. Biophys. Acta.* 1098:271–274.

MSI. 1997. QUANTA 97. Molecular Simulations Inc., Burlington, Massachusetts.

Nagae, H., T. Kakitani, T. Katohi, and M. Mimuro. 1993. Calculation of the excitation transfer matrix elements between the S_2 or S_1 state of carotenoid and the S_2 or S_1 state of bacteriochlorophyll. *J. Chem. Phys.* 98:8012–8023.

Norris, B., and D. Miller. 1994. Nucleotide sequence of a cDNA clone encoding the precursor of the peridinin-chlorophyll *a*-binding protein from the dinoflagellate *Symbiodinium* sp. *Plant Mol. Biol.* 24:673–677.

Pariser, R. 1956. Theory of the electronic spectra and structure of the polyacenes and of alternant hydrocarbons. *J. Chem. Phys.* 24:250–268.

Pariser, R., and R. G. Parr. 1953. A semi-empirical theory of the electronic spectra and electronic structure of complex unsaturated molecules. I. *J. Chem. Phys.* 21:466–471.

Pilch, M., and M. Pawlikowski. 1998. Circular dichroism (CD) study of peridinin-chlorophyll *a* protein (PCP) complexes from marine dinoflagellate algae. *J. Chem. Soc. Faraday Trans.* 94:227–232.

Pople, J. A. 1953. Electron interaction in unsaturated hydrocarbons. *Trans. Faraday Soc.* 42:1375–1385.

Ritz, T., X. Hu, A. Damjanović, and K. Schulten. 1998. Excitons and excitation transfer in the photosynthetic unit of purple bacteria. *J. Luminescence* 76–77:310–321.

Scholes, G., R. Harcourt, and G. Fleming. 1997. Electronic interactions in photosynthetic light-harvesting complexes: the role of carotenoids. *J. Phys. Chem. B.* 101:7302–7312.

Schulten, K., and M. Karplus. 1972. On the origin of a low-lying forbidden transition in polyenes and related molecules. *Chem. Phys. Lett.* 14: 305–309.

Shreve, A. P., J. K. Trautman, T. G. Owens, and A. C. Albrecht. 1991. Determination of the S_2 lifetime of β-carotene. *Chem. Phys. Lett.* 178: 89–96.

Song, P.-S., P. Koka, B. Prezelin, and F. Haxo. 1976. Molecular topology of the photosynthetic light-harvesting pigment complex, peridinin-chlorophyll *a*-protein, from marine dinoflagellates. *Biol. Cybernetics.* 15:4422–4427.

Tavan, P., and K. Schulten. 1986. The low-lying electronic excitations in long polyenes: A PPP–MRD–CI study. *J. Chem. Phys.* 85:6602–6609.

Zhang, J.-P., R. Fujii, P. Qian, T. Inaba, T. Mizoguchi, and Y. Koyama. 2000. Mechanism of the carotenoid-to-bacteriochlorophyll energy transfer via the S_1 state in the LH2 complexes from purple bacteria. *J. Phys. Chem. B.* 104:3683–3691.